Diet Processing and Nutrient Composition Drive Divergent Obesity Phenotypes in Wistar Rats

Pedro Rocha Tenorio. Department of Physiological Sciences, State University of Londrina, Londrina, Brazil. rocha.pedro.tenorio@uel.br ORCID: 0000-0003-1812-4792

Gabriel Smolak Sobieski e Silva. Department of Physiological Sciences, State University of Londrina, Londrina, Brazil. ORCID: 0000-0002-9944-3519

Débora Hipólito Quadreli. Department of Pathology Sciences, State University of Londrina, Londrina, Brazil. ORCID: 0009-0000-8323-3712

Glaura Scantamburlo Alves Fernandes. Department of General Biology, State University of Londrina, Londrina, Brazil. ORCID: 0000-0002-6043-1131

Fabio Goulart de Andrade. Department of Histology, State University of Londrina, Londrina, Brazil. ORCID: 0000-0002-0206-4986

ABSTRACT

Purpose
This study aimed to investigate whether food processing, alone or combined with high-fat/high-sugar content, promotes obesity, metabolic syndrome (MtS), and oxidative stress in adult rats.

Methods
Male Wistar rats were fed for 10 weeks with either a commercial grain-based diet (C/GB), a balanced semi-purified diet (B/SP), or a high-fat/high-sugar semi-purified diet (HFS/SP). Murinometric, metabolic, histological, and oxidative parameters were assessed. Multivariate clustering and principal component analysis (PCA) were used to identify metabolic phenotypes.

Results
Despite similar caloric intake, B/SP-fed rats developed increased adiposity and body weight without metabolic disturbances. In contrast, HFS/SP-fed animals exhibited hyperglycemia, dyslipidemia, hepatic steatosis, and marked systemic oxidative stress despite no excess weight gain. Clustering analysis identified three partially overlapping phenotypes: a metabolically healthy profile (C/GB), an intermediate profile resembling metabolically healthy obesity (B/SP), and a distinct metabolically unhealthy non-obese group (HFS/SP). The overlap between B/SP and C/GB groups suggests a transitional zone rather than sharply defined states. Oxidative stress markers and hepatic steatosis were strongly associated with metabolic impairments, especially in the HFS/SP group.

Conclusion
Diet composition and processing play a decisive role in shaping metabolic and redox phenotypes, independent of caloric intake or body mass. These findings support the fuel partitioning hypothesis and expand the translational relevance of Wistar rats by demonstrating intermediate and overlapping metabolic states resembling human obesity subtypes not previously documented, highlighting the potential of male Wistar rats as a versatile model to study diverse obesity-related metabolic phenotypes relevant to human conditions.

KEYWORDS

Semi-purified diet; Obesity; Metabolically Healthy Obesity; Normal-Weight Obesity Syndrome; Oxidative Stress; Fuel Partitioning Model.

INTRODUCTION

The global prevalence of obesity has been steadily increasing since 1975 [1], with its economic burden reaching an estimated $1.88 trillion in 2019 [2] and contributing to 8.9% of global mortality [3]. Recognized as a pandemic by the World Health Organization in 1995, obesity is projected to affect 51% of the global population by 2030, thus posing one of the 21st century's most pressing public health challenges [4].

The most widely accepted pathophysiological mechanism of obesity involves excessive adipose tissue accumulation coupled with impaired oxidative capacity. This imbalance results in elevated production of reactive oxygen species (ROS), primarily within mitochondria and cellular membranes. Initially localized, oxidative stress (OS) can become systemic as ROS disseminate via the bloodstream. In insulin-sensitive organs such as the liver, systemic OS disrupts metabolic homeostasis, impairs insulin

signaling, and promotes hypercholesterolemia and insulin resistance. These metabolic disturbances establish a positive feedback loop that can culminate in steatotic liver disease [5] and metabolic syndrome (MtS), including comorbidities such as type 2 diabetes (T2D) and cardiovascular disease [6].

Obesity is a multifactorial condition, with dietary habits playing a crucial role in its pathogenesis[6]. Excessive consumption of sugars and fats has been demonstrated to promote adipose tissue expansion and ROS generation through glycation and lipotoxicity [6, 7]. Ultra-processed food consumption has also been implicated in disease development, although the epidemiological evidence remains inconclusive [8]. Animal models frequently employed in the study of obesity and MtS rely on purified diets (PDs), composed of standardized ingredients such as isolated proteins, refined carbohydrates, and purified fats [9], mimicking ultra-processed human diets and offering experimental reproducibility [10]. However, such diets are deficient in biologically active compounds, such as phytochemicals, that can modulate digestion and metabolism [11], thereby limiting their physiological representativeness and translational relevance [12].

Comparative studies of PDs and natural ingredient diets yield conflicting results. While some studies demonstrate PD-induced metabolic harm [13], others report no adverse effects [14] or even improvements relative to chow diets [15]. Semi-purified diets (SP), combining natural and refined ingredients, may offer greater translational relevance, though research remains scarce. While one study links SDs to steatosis and hypercholesterolemia in pregnant rats [16], other highlights genotype-dependent metabolic responses in mice [17]. Notably, no study has explored OS dynamics in SD-fed models. Although high-fat/high-sugar diets are widely used to induce metabolic dysfunction in rodents [7], it remains unclear whether food processing itself, independent of macronutrient excess, contributes to these pathologies.

To address this knowledge gap, this study investigates whether food processing alone (by comparing natural-ingredient and semi-purified balanced diets) or in combination with high-fat/high-sugar content (semi-purified hypercaloric diet) promotes obesity, comorbidities, and oxidative stress in adult rats.

METHODS

Animal Housing and Management.

Given the lack of consensus on rodent obesity classification and the high inter-study variability in Wistar rat weight gain, a conservative estimate of a 25% excess weight gain over a 10-week experimental period was adopted as the benchmark [18]. This is equivalent to a mean additional weight gain of 20 g in adult animals, based on the characteristics of the animals housed in our vivarium. Assuming a standard deviation of 10 g, with $\alpha = 0.05$ and statistical power set at 0.80, the minimum required sample size was calculated as $n = 4.3$ animals per group [19].

Fifteen 90-day-old male Wistar rats were housed in groups of 2-3 animals per cage under controlled conditions (22 ± 2ºC, 12 h light/dark cycle) with *ad libitum* access to water and food for a period of 73 days. Body weight, food intake, and water consumption were monitored twice-weekly using the residual intake method and adjusted for the number of animals per cage. The rats were randomly assigned to three dietary groups (n = 5): commercial grain base diet (C/GB) fed (Nuvilab CR1®, Quimtia, Brazil), balanced semi-purified Diet (B/SP), and high-fat/high-sugar semi-purified diet (HFS/SP).

On the 74th day, following a 6-8 hour fast, the animals were anesthetized via intraperitoneal (*i.p.*) administration of ketamine (100 mg/kg) and xylazine (10 mg/kg). The nasal-anal length was

measured, and blood samples were collected from the inferior vena cava into tubes containing a coagulation activator (FristLab, Brazil). The liver, inguinal adipose tissue (iAt), and retroperitoneal adipose tissue (rAt) were dissected, washed in ice-cold PBS, and processed accordingly. The collected blood was centrifuged at 12,000 × g for 10 minutes, after which the serum was separated and stored at -20°C.

Diet Preparation and Composition

The SP were prepared on a weekly basis in the laboratory. The dry ingredients were mixed with water in a kitchen blender, oven-dried at 65°C for 72 hours, and stored in sealed containers. Nutrient composition was formulated in accordance with NRC-95G guidelines to prevent nutritional deficiencies[20]. Table 1 presents the nutrient composition data. The estimated glycemic load for the C/GB diet was 29, for the B/SP was 38.5 and for the HFS/SP was 13.4 [21].

Table 1. Nutritional Composition of Different Diets

	C/GB	B/SP	HFS/SP
Soy Protein Isolate (g)	-	100	100
Wheat Gluten (g)	-	25	25
Dried Whole Egg (g)	-	25	25
Corn Starch (g)	-	474	-
Maltodextrin (g)	-	100	100
Degermed Corn Meal (g)		100	100
Defatted Soybean Meal (g)		-	-
Sucrose (g)	-	-	100
Wheat Bran (g)		50	50
Psyllium Husk (g)	-	25	25
Coconut Flour (g)	-	100	100
Brazilian Nut Flour (g)	-	5	5
Lard (g)	-	-	155
Soybean Oil (g)		-	-
Brew's Yeast (g)	-	25	25
Mineral Mix (g)		22	22
Vitamin Mix (g)		18	18
Total (g)	-	1069	850
Energy (kcal/kg)	3468	3697	4625
Carbohydrates (g/kg) (% kcal)	525 (66)	597 (71)	364 (36)
Added Sugars (g/kg) (% kcal)	0	0	117 (10)
Lipids (g/kg) (% kcal)	40 (10)	57 (14)	254 (49)
Protein (g/kg) (% kcal)	223 (24)	151 (15)	188 (15)
Fiber (g/kg)	67	72	86
Cholesterol (mg/kg)	0	397	673
Vitamin E (mg/kg)	27	47	60

Murinometric and Dietary Parameters

The data pertaining to body weight and food intake were utilized to calculate food efficiency. The adiposity index was calculated as rAt+iAt/the body weight, while the visceral/subcutaneous ratio (vAt/sAt) was expressed as rAt/iAt [22].

Metabolic Profile

Immediately following anesthesia, fasting capillary blood glucose levels were measured from the tail vein using a glucometer (G-Tech Lite®, MEDFARM, Brazil). Medium-term glycemic control was assessed by quantifying serum fructosamine, and lipid profile variables (triglycerides, glycerol, total cholesterol, non-HDL) were measured using commercial kits.

Liver Histology

Liver tissue samples were fixed in 4% paraformaldehyde for 24 hours, embedded in paraffin, and sectioned at 5 µm for histological analysis. Sections were stained with hematoxylin and eosin and evaluated to determine the presence of metabolic-associated steatohepatitis (MASH) [23]. Histological images were captured using a BA310MET-T light microscope (Motic, China) equipped with a Moticam A5 digital camera and analyzed with ImageJ software (v1.53, National Institutes of Health, USA).

Systemic Serum Oxidative Profile

Superoxide dismutase (SOD) activity was assessed based on its ability to inhibit superoxide anion generation, while catalase (CAT) activity was quantified by monitoring the decomposition rate of hydrogen peroxide [24]. Non-enzymatic antioxidant defenses were assessed through ferric-reducing antioxidant power (FRAP) [25], total glutathione (GT), reduced glutathione (GSH), and glutathione disulfide (GSSG) levels [26]. Oxidative damage was assessed via lipid peroxidation (LOOH) [27], protein carbonylation concentration (PCO) [28], and total reactive oxygen species (TOS) using a modified FOX-1 assay [29]. All spectrophotometric measurements were performed in a Multiskan™ FC Microplate Photometer (Thermo Fisher Scientific, USA; Model 51119000).

Statistical Analysis

Normality and homogeneity of variances were assessed using the Shapiro-Wilk and Brown-Forsythe tests, respectively. For datasets with normally distributed residuals, one-way ANOVA followed by Tukey's HSD post hoc test was used. In cases of heteroscedasticity, Welch's ANOVA with Games-Howell correction was applied. For data with non-normal residuals, log transformation was performed, followed by reassessment of normality and variance homogeneity; if assumptions were met, ANOVA or Welch's methods were applied accordingly. When normality was not achieved even after transformation, the Kruskal-Wallis test with Dunn's multiple comparisons post hoc was employed. Steatosis scores and MASH prevalence were analyzed using Fisher's exact test. Clustering analysis was conducted using hierarchical clustering with the Ward.D2 linkage method and Manhattan distance metric. Statistical significance was set at $p<0.05$. All analyses were performed in RStudio (v4.2, Posit, USA) using the 'onewaytests', 'cluster', 'factoextra', 'pheatmap', and 'ggplot2' packages.

RESULTS

Murinometric and Dietary Parameters

Initial body weights were comparable across groups, confirming similar baseline conditions. Final body weight and total weight gain were significantly higher in the B/SP group compared to both C/GB and HFS/SP, with no difference between C/GB and HFS/SP (Fig. 1a-c). Liver weight did not vary significantly among groups (Fig. 1d).

Marked differences in adipose tissue distribution were observed across dietary interventions. iAT was significantly elevated in the B/SP group compared to both C/GB and HFS/SP groups, while the HFS/SP group also exhibited higher iAT than the C/GB group (Fig. 1e). rAT was similarly increased in both the B/SP and HFS/SP groups relative to C/GB (Fig. 1f). The adiposity index was significantly higher in the B/SP group compared to both C/GB and HFS/SP groups, with the HFS/SP group also showing a significant increase relative to C/GB (Fig. 1g). The vAt/sAt ratio was significantly lower in the B/SP group, indicating a shift toward subcutaneous fat deposition (Fig. 1h).

Fig. 1 Effects of dietary interventions on morphometric parameters: Initial body weight (a), final body weight (b), body weight gain (c), liver weight (d), inguinal adipose tissue relative weight (e), retroperitoneal adipose tissue relative weight (f), adiposity index (g), visceral-to-subcutaneous adipose tissue ratio (h). Diet groups: C/GB = commercial grain-based diet, B/SP = balanced semi-purified diet, HFS/SP = high-fat high-sugar semi-purified diet. Statistical analysis: One-way ANOVA with Tukey's HSD post hoc or Welch's ANOVA with Games–Howell correction. Data are presented as box plots as median and interquartile ranges; white dots indicate group means.

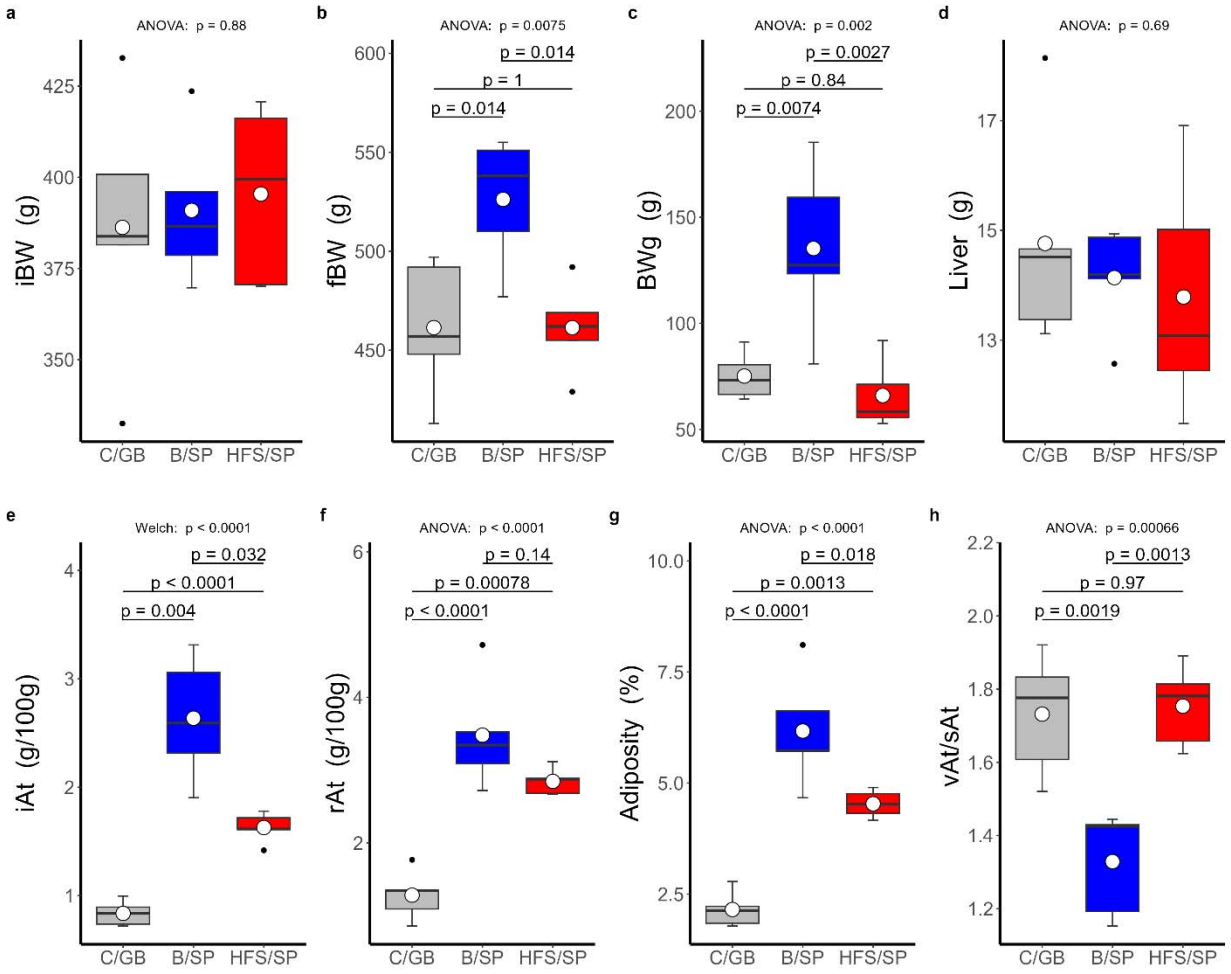

Water intake was significantly lower in both the B/SP and HFS/SP groups in comparison to the C/GB group, with the HFS/SP group exhibiting an even greater reduction compared to the B/SP group. The HFS/SP group demonstrated the lowest total and mean daily chow intake when compared to both the C/GB and B/SP groups. Although caloric intake was similar between C/GB and B/SP, food efficiency was significantly higher in B/SP animals. In contrast, no significant difference in food efficiency was observed between the C/GB and HFS/SP groups (Fig. 2).

Fig. 2 Dietary parameters among different diets. Diet groups: C/GB = commercial grain-based diet, B/SP = balanced semi-purified diet, HFS/SP = high-fat high-sugar semi-purified diet. Statistical analysis: One-way ANOVA with Tukey's HSD post hoc, Welch's ANOVA with Games–Howell correction or Kruskal-Wallis with Dunn's multiple comparisons post hoc. Data are presented as box plots as median and interquartile ranges; white dots indicate group means.

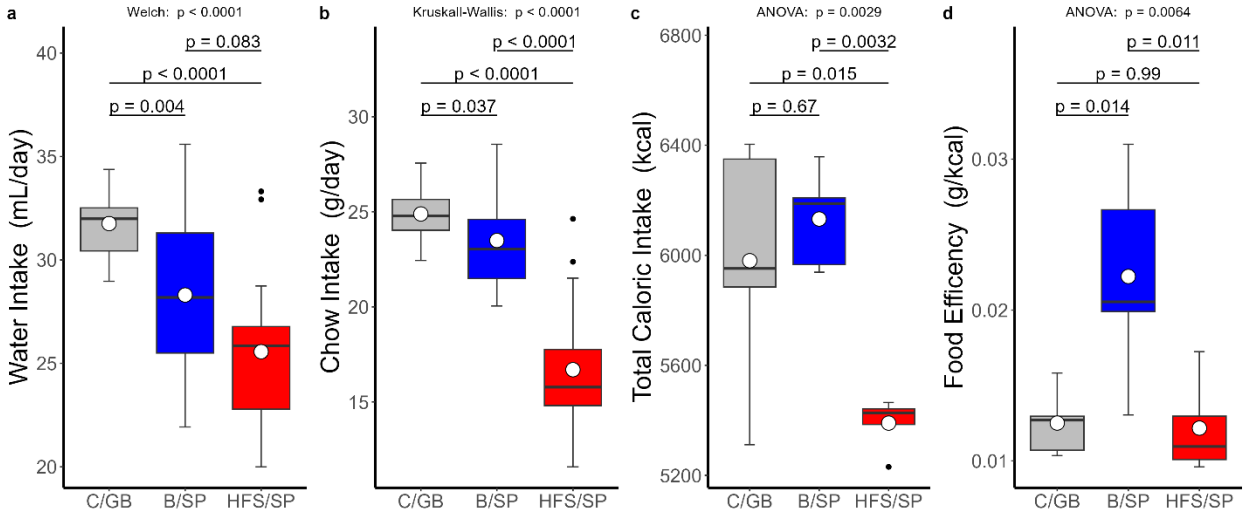

Metabolic Parameters

Fasting blood glucose and fructosamine levels were significantly elevated in the HFS/SP group in comparison to the C/GB and B/SP groups. However, no significant differences were observed between the C/GB and B/SP groups (Fig. 3a, b). Serum triglycerides were highest in the HFS/SP group, and lowest in B/SP animals, which also showed a significant reduction compared to C/GB. Glycerol concentrations were elevated in the B/SP group compared to both C/GB and HFS/SP, whereas the HFS/SP group exhibited reduced levels relative to C/GB (Fig. 3c, d). Conversely, both total cholesterol and non-HDL cholesterol levels were elevated in the HFS/SP group relative to C/GB and B/SP, while B/SP exhibited an increase only in total cholesterol compared to C/GB (Figure 3e, f).

Fig. 3 Blood metabolic profiles: Capillary fasting glucose (a), serum fructosamine/albumin concentration (b), serum triglycerides concentration (c), serum glycerol concentration (d), total cholesterol concentration (e), non-HDL cholesterol concentration (f). Diet groups: C/GB = commercial grain-based diet, B/SP = balanced semi-purified diet, HFS/SP = high-fat high-sugar semi-purified diet. Statistical analysis: One-way ANOVA with Tukey's HSD post hoc. Data are presented as box plots as median and interquartile ranges; white dots indicate group means.

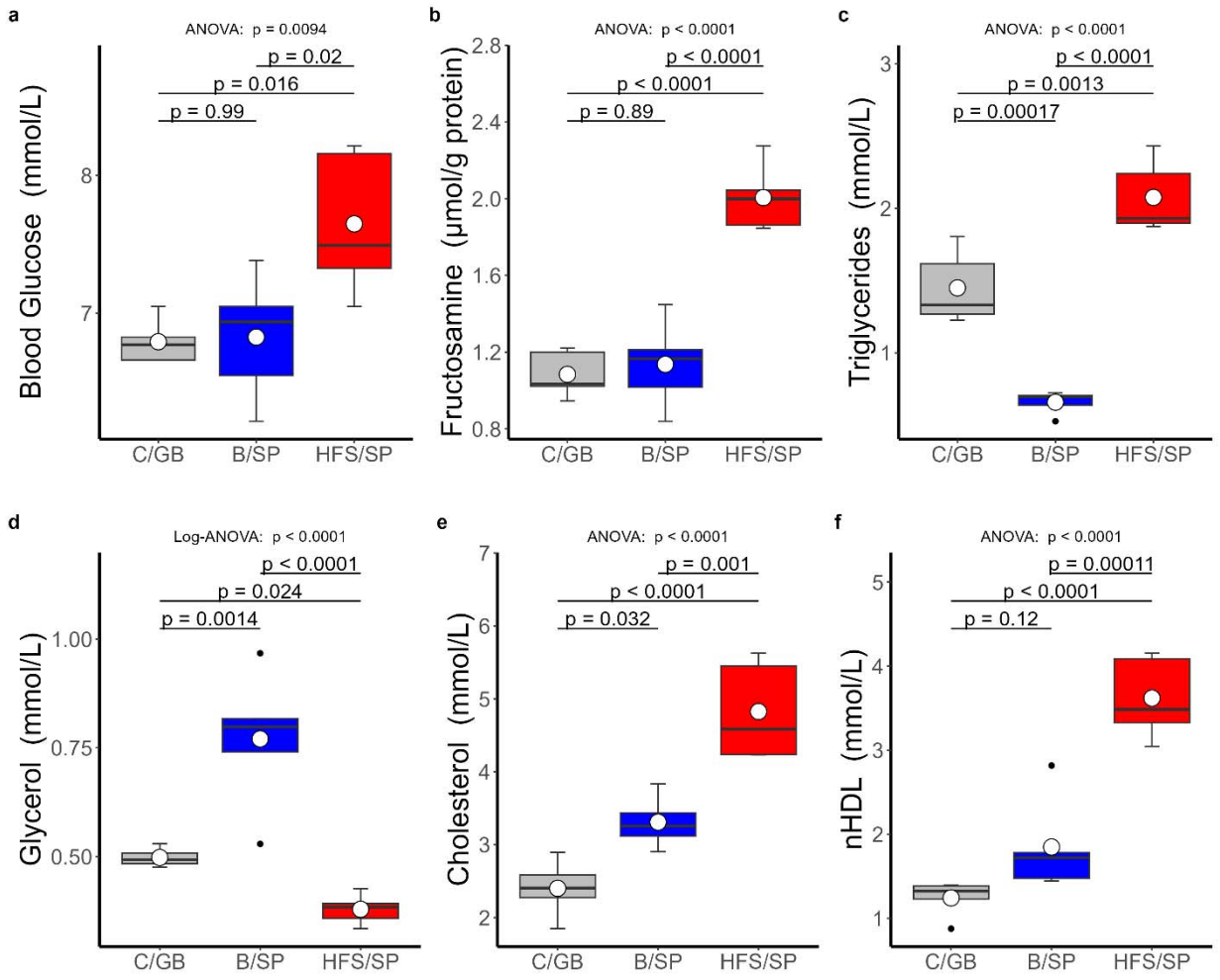

Liver Histology

Histological analysis of liver tissue revealed different patterns of steatosis between the dietary groups. The B/SP group showed sparse macrovesicular lipid droplets, whereas the HFS/SP group showed extensive areas of mixed macrovesicular and microvesicular steatosis (Fig. 4a). A significant association was observed between dietary intervention and steatosis severity (Fisher's exact test, p=0.045; Fig. 4b). Pairwise comparisons showed a higher steatosis score in the HFS/SP group compared to the C/GB group (p=0.048, V=0.89). In addition, a statistical trend was also observed between the HFS/SP and B/SP groups (p=0.064, V=0.86); although not reaching conventional significance, the large effect size suggests potential clinical significance. No significant differences were observed between the C/GB and B/SP groups. Furthermore, confirmation of MASH was confirmed only in the HFS/SP group, which differed significantly from both C/GB and B/SP (Fig. 4c)

Fig. 4 Histological evaluation and severity scoring of steatosis and occurrence of metabolic-associated steatohepatitis. Representative hematoxylin and eosin-stained liver sections (a), contingency table showing the distribution of steatosis severity scores across groups (b), contingency table showing the confirmation of Metabolic-Associated Steatohepatitis (c). Statistical analysis: Fisher's exact test; [a] indicates p<0.05 compared to

C/GB, [b] indicates $p<0.05$ compared to B/SP. Scale bar = 25 µm; (↖) arrows indicate lipid droplet, (▲) arrowhead indicates ballooning.

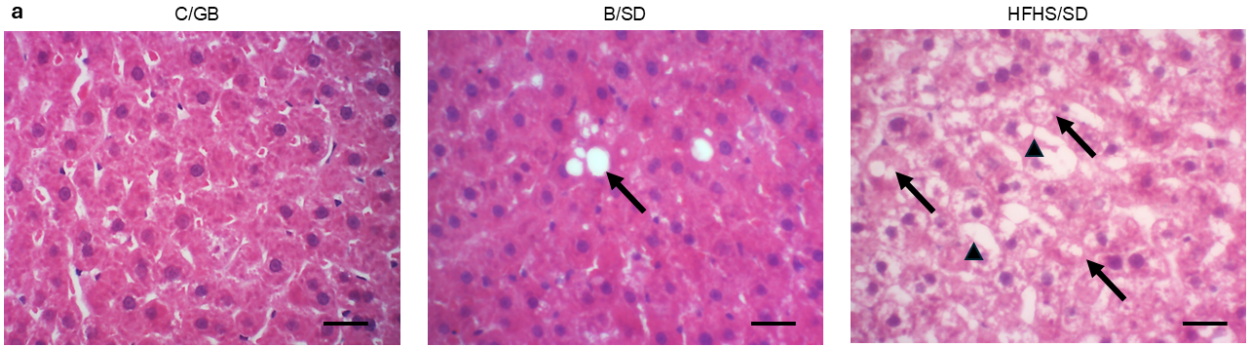

b

Steatosis

	C/GB	B/SP	HFHS/SP[a]
Absent	4	3	0
Mild	1	2	1
Moderate	0	0	2
Severe	0	0	2

c

Metabolic-Associeted Steatohepatites

	C/GB	B/SP	HFHS/SP[a,b]
Health	5	5	1
MASH	0	0	4

Systemic Serum Oxidative Profile

Enzymatic antioxidant markers exhibited diet-induced modulations. Specifically, SOD activity was similarly elevated in B/SP and HFS/SP, with no difference between them. However, no significant differences were observed between the two experimental diets (Fig. 5a). CAT activity exhibited an increase in the HFS/SP group and, to a lesser extent, in the B/SP group compared to the C/GB group (Fig. 5b). FRAP was similarly elevated in both B/SP and HFS/SP groups versus C/GB (Fig. 5c). While there were no significant differences in glutathione transferase (GT) and glutathione (GSH) levels among the groups, there was a significant reduction in GSSG in B/SP animals compared to HFS/SP. The GSSG/GSH ratio, a key indicator of OS, exhibited a substantial increase in the HFS/SP group (Fig. 5d-g). Furthermore, Oxidative damage markers (LOOH, PCO, TOS) were significantly elevated in the HFS/SP group compared to both C/GB and B/SP. However, there were no significant differences observed between the C/GB and B/SP groups (Fig. 5h-j).

Fig. 5 Oxidative stress and antioxidant responses to grain base and semi purified diets. Superoxide dismutase (SOD) activity (a), catalase (CAT) activity (b), ferric reducing antioxidant power (FRAP) in ascorbic acid equivalent (c), total glutathione (GT) concentration (d), reduced glutathione (GSH) concentration (e), oxidized glutathione (GSSG) concentration (f), GSSG/GSH ratio (g), lipid hydroperoxides (LOOH) in H_2O_2 equivalent (h), carbonylated protein (PCO) concentration (i), total oxidative species (TOS) in H_2O_2 equivalent (j). Diet groups: C/GB = commercial grain-based diet, B/SP = balanced semi-purified diet, HFS/SP = high-fat high-sugar semi-purified diet. Statistical analysis: One-way ANOVA with Tukey's HSD post hoc, or Welch's ANOVA with Games–Howell correction. Data are presented as box plots as median and interquartile ranges; white dots indicate group means.

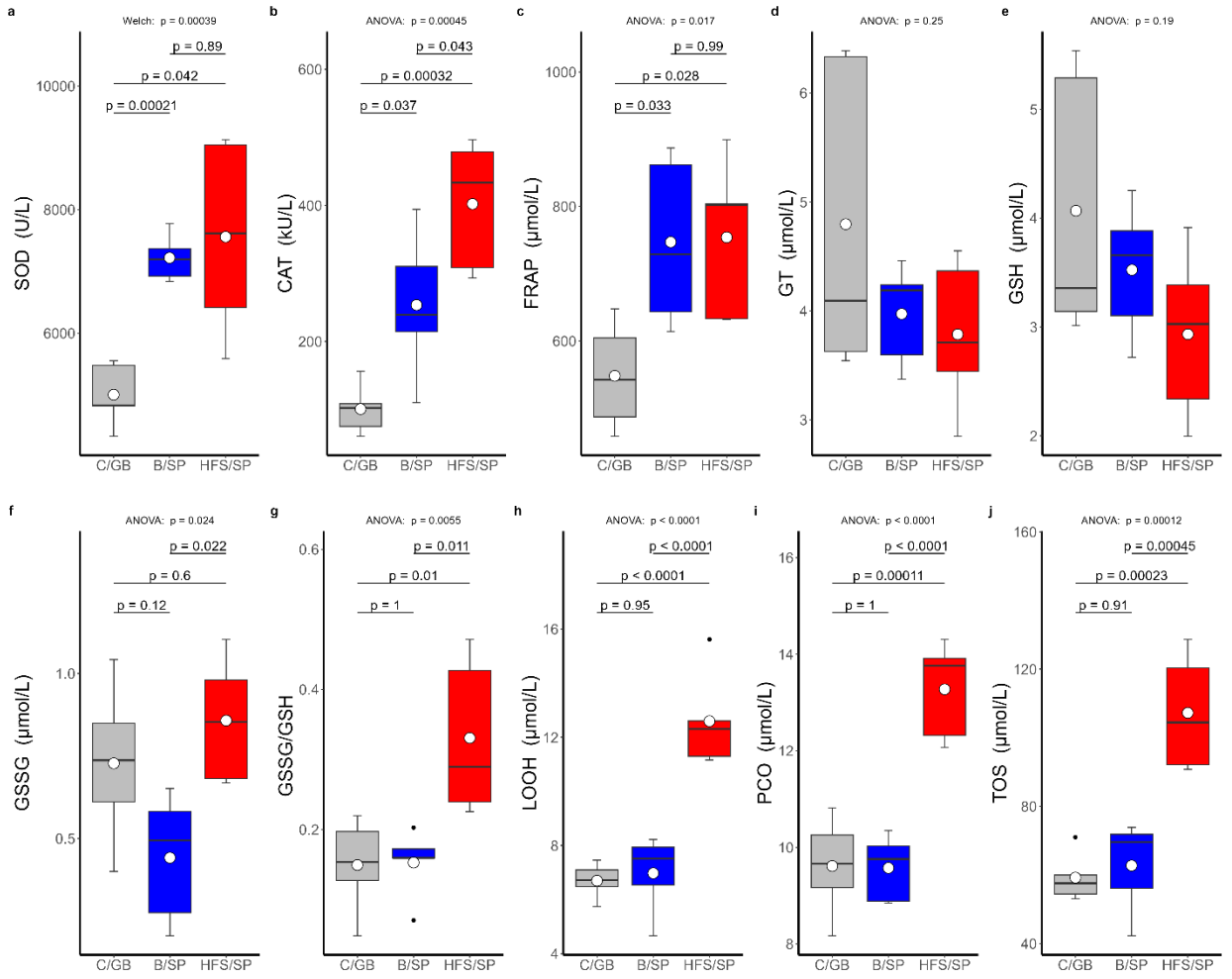

Unsupervised Clustering

Hierarchical clustering based on metabolic, oxidative, and morphometric variables identified three distinct clusters, with partial overlap between two of them. The primary drivers of cluster differentiation included oxidative stress markers (LOOH, PCO, TOS), metabolic indicators (glycerol, fructosamine, non-HDL cholesterol, and total cholesterol), and murinometric variables (weight gain, iAT, final body weight, and steatosis degree) (Fig. 6a). Cluster 3, consisting exclusively of HFS/SP animals, exhibited the highest levels of oxidative and metabolic stress, alongside severe hepatic steatosis. Cluster 2, comprising four B/SP animals, displayed an intermediate phenotype characterized by altered lipid metabolism, enhanced antioxidant responses, and increased weight and adiposity. Cluster 1 included all C/GB animals and one B/SP animal, representing the most metabolically stable and redox-balanced profile (Fig. 6b). The clustering robustness was supported by an average silhouette width of 0.43, indicating that Cluster 3 formed a well-separated and coherent group, while Clusters 1 and 2 showed some overlap (Fig. 6c). Principal component analysis further corroborated these findings, revealing distinct spatial segregation of the HFS/SP group and a notable overlap between C/GB and B/SP groups (Fig. 6d).

Variable-wise hierarchical clustering revealed strong correlation structure patterns linking MtS markers with OS profiles (Figure 5B). A prominent cluster included cholesterol, blood glucose, and steatosis, which were tightly associated with redox imbalance markers such as the fructosamine, GSSG/GSH ratio and LOOH. Adjacent to this cluster, additional OS parameters (CAT, TOS, and PCO) formed a related group, reinforcing the coordinated disruption of redox homeostasis in metabolically compromised animals, particularly within the HFS/SP group.

Fig. 6 Unsupervised clustering analysis: Key variable contributions to clusters (a), heatmap with hierarchical clustering displaying individual z-score-scaled values, row dendrogram represents clustering based on Manhattan distance, while the column dendrogram reflects correlation-based distance (b), silhouette plot indicating clustering quality (c), principal component analysis of variables with cluster overlay using a multivariate t-distribution (d). Colors: Cluster 1 = light red, Cluster 2 = green, Cluster 3 = light blue. Diet groups: C/GB = commercial grain-based diet, B/SP = balanced semi-purified diet, HFS/SP = high-fat high-sugar semi-purified diet. Symbols: C/GB = black dot (⬤), B/SP = blue triangle (▲), HFS/SP = red diamond (◆).

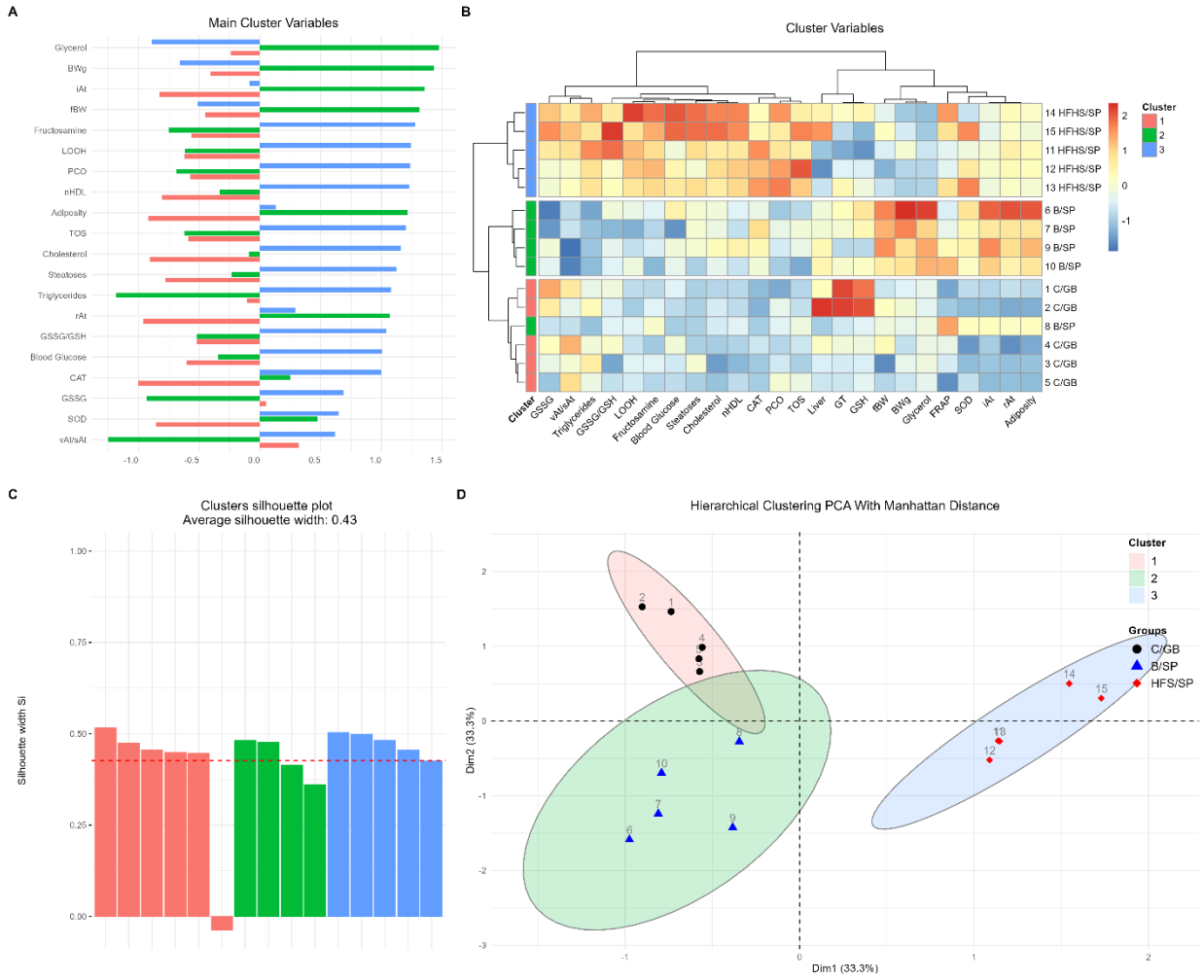

DISCUSSION

BMI has traditionally served as the primary metric for assessing obesity-related health risks, positioning body weight as the principal indicator of metabolic dysfunction. However, emerging perspectives increasingly recognize that the pathological accumulation and distribution of adipose tissue provide more precise predictors of metabolic risk. While this conceptual shift has refined clinical assessment, it remains inadequate to explain the full spectrum of obesity-related comorbidities. Our findings contribute to this evolving understanding by demonstrating that dietary composition and processing, independent of total caloric intake or body weight, play a decisive role in shaping distinct metabolic phenotypes and systemic oxidative profiles.

High-fat purified diets are widely used in rodent models of diet-induced obesity due to their low satiety and hyperphagic effects [10]. However, animals on the HFS/SP diet consumed fewer calories than controls yet gained similar weight. Although unexpected, comparable outcomes have been reported under high-fat diets with lower fat content (35% vs. 49%) and micronutrient profiles mimicking human intake rather than rodent-specific recommendations [30]. Notably, despite reduced caloric intake and the absence of excess weight gain, HFS/SP animals developed significant visceral fat accumulation and can be classified as obese based on fat distribution rather than total body mass [31].

Fasting glucose levels above 7 mmol/L, alongside elevated fructosamine, indicate sustained hyperglycemia consistent with T2D in the HFS/SP group. Impaired fasting glucose suggests hepatic and muscular insulin resistance [18], in combination with low serum glycerol, indicating suppressed lipolysis, particularly from visceral adipose tissue, the primary source of circulating lipids [32], implies preserved insulin sensitivity in white adipose tissue [33]. This profile supports a shift toward energy storage redistribution, favoring adipose tissue, aligning with the fuel partitioning model of obesity. In this model, intrinsic defects in energy distribution lead to metabolic dysfunction, where excessive body weight is a consequence rather than the primary cause [34].

In contrast to high-fat diets, the B/SP diet led to greater body weight and adiposity than the other groups, despite similar caloric intake. While it is well-established that carbohydrate-rich diets alone typically do not induce obesity without forced feeding or additional metabolic challenges [35], our findings show that *ad libitum* intake of a carbohydrate-predominant, semi-purified diet can lead to obesity in rodents. This unexpected outcome may be partially explained by increased metabolizable energy from the processed SP diets[36], and the partial substitution of fat source by coconut fat, a source of medium chain fat acids with easy and rapid absorption [37].

A higher lipid and carbohydrate digestibility enhancing energy efficiency due to the reduction of phytochemicals, may also be expected [38, 39]. Additionally, the high glycemic load of the B/SP diet may cause postprandial glucose spikes, stimulating glucose to be transported preferentially into adipose tissue and promoting lipogenesis, fat accumulation, and weight gain [40]. Together, these mechanisms may explain the increase in adiposity and body weight, despite no excess caloric intake. In summary, improved macronutrient availability and rapid absorption lead to greater fat deposition and body mass.

The T2D, increased adiposity, and elevated triglyceride and cholesterol levels, found in HFS/SP animals support classifying these animals as exhibiting MtS [31]. In contrast, B/SP-fed animals showed no pathological changes in serum metabolic profiles. This absence of metabolic dysfunction may be partly explained by a preferential accumulation of subcutaneous rather than visceral fat, a distribution pattern linked to enhanced fat mobilization, reduced strain on internal organs, and overall metabolic resilience [32]. Additionally, the inclusion of coconut fat derived from coconut flour in the B/SP diet may

have contributed to these protective effects, as previous studies have shown that coconut fat attenuates disruptions in glucose homeostasis in MtS dietary models by increasing serum levels of non-esterified fatty acids without adversely affecting cholesterol levels [37].

In addition to the high-fat content of diet, other nutritional factors may have contributed to these metabolic profiles. Fructose content of the diets may be a determinant factor, while the refined cornstarch in the B/SP diet, composed solely of glucose polymers, can trigger a strong postprandial insulin response, glucose has not been shown to induce insulin resistance in rats. In contrast, sugar-induced insulin resistance is primarily linked to fructose intake and its ability to induce hepatic metabolic dysregulation and steatoses [40], dietary element presents only in the HFS/SP diet. Dietary cholesterol is another factor implicated in insulin resistance, primarily via hepatic steatosis [41] and visceral adipose inflammation [42]. Although the cholesterol levels in this study (0.04% and 0.07%) were well below the doses typically linked to metabolic dysfunction in rodents (0.5%–1%), its combination with dietary fructose may have exerted a synergistic effect, amplifying metabolic disturbances beyond the impact of either component alone.

Although adipose dysfunction is a central feature of obesity-related metabolic changes [31], our findings suggest that adiposity alone does not fully explain the observed outcomes. The fat redistribution in B/SP animals may partly underlie their metabolically protected profile; however, the similar visceral adipose tissue between the two SP groups indicates other mechanisms for metabolic disturbance. Oxidative stress is a central mechanism in obesity-related comorbidities [6]. Systemic oxidative status reflects overall redox balance and serves as both an indicator of physiological disturbance and a marker of oxidative dissemination [43]. Since the redox system is influenced by nutritional status, obesity, and their comorbidities [44], we assessed systemic oxidative stress to clarify its role in the metabolic alterations observed.

Certain nutrients, such as vitamin E, enhance antioxidant defenses by supporting non-enzymatic antioxidants and boosting enzymes like SOD and CAT [45]. The commercial chow used in the C/GB group have been previously demonstrated to inadequately support hepatic antioxidant defenses, possibly due to suboptimal vitamin E content, leading to elevated oxidative damage markers compared to standardized purified diets [46]. In contrast, the SPs diets provided more than twice the vitamin E in C/GB, which may explain the stronger antioxidant response in SP-fed animals.

Dietary lipids also modulate antioxidant enzyme expression. For example, cholesterol enhances the synthesis of the mitochondrial isoform of SOD [47], while dietary fat selectively increases CAT levels[48]. Antioxidant responses to lipid overload may result from lipotoxicity and mitochondrial dysfunction, which elevate ROS production. Fructose, too, increases ROS via mitochondrial overproduction, NADPH oxidase activation [6], and enhanced purine degradation [49]. Additionally, excessive sugar fosters protein glycation, resulting in ROS formation via advanced glycation end-products[50], consistent with elevated fructosamine in our HFS/SP group.

The HFS/SP phenotype diverges from conventional diet induced obesity models, resembling more closely those induced by hypothalamic lesions [34] or monosodium glutamate-induced hypothalamic cytotoxicity [51], where fat accumulation occurs independent of hyperphagia, we speculate that an oxidative alteration in regions of metabolic control of the hypothalamus may explain the phenotype found in HFS/SP animals. In fact, high-fat diets have been previously shown to induce direct hypothalamic oxidative stress [52] and indirect by systemic oxidative stress [43] particularly in the

arcuate nucleus. This hypothalamic stress results in impairing melanocortin signaling which can favor adipose tissue deposition with and without hyperphagia, reinforcing the hypothesis of energy partitioning defect [34, 52].

Beyond dietary influences, our findings reinforce the central role of metabolically active organs, particularly the liver, in regulating whole-body homeostasis and driving metabolic dysfunction[53]. The liver, capable of generating ROS in response to endogenous and exogenous stimuli [54], emerged as a key organ in this model. Hepatic steatosis showed the strongest association with metabolic impairment, especially in glucose and lipid regulation. Similarly, human studies report that adiposity primarily contributes to metabolic disease when accompanied by increased liver fat [55]. Furthermore, the clustering patterns observed here emphasize the combined impact of diet and hepatic function on oxidative stress, aligning with lipotoxicity-driven mechanisms associated with ectopic fat accumulation and insulin resistance [6]. These results suggest that liver health and diet may be more critical than adiposity alone in determining metabolic disease risk and phenotypic diversity.

The distinct metabolic and oxidative profiles observed, particularly the separation between the C/GB and HFS/SP groups and the intermediate features of B/SP animals, closely resemble clinical obesity subtypes such as metabolically healthy obesity (MHO) [56] and normal-weight obesity syndrome (NWOS) [57], also known as metabolically unhealthy non-obese [58]. MHO is considered a transient state that often progresses to metabolic complications; thus, the ~10-week obesity induction period in this study may not have been sufficient to cause glycolipid alterations through adiposity alone [58]. Although 10 weeks is typically adequate for metabolic dysfunction to emerge in male Wistar rats, such changes are usually linked to diets rich in fat or sugar. Our findings indicate that diet composition, rather than excess adiposity alone, are the primary driver of rapid metabolic alterations, offering insight into the origins of the MHO phenotype [18].

The dissociation between obesity and metabolic complications, seen in phenotypes like MHO and NWOS, has been reported in other animal models, but is usually strain specific. Wistar rats are typically described as either developing metabolic syndrome with obesity or remaining metabolically healthy. Remarkably, this study is the first, to our knowledge, to identify both obese animals without metabolic dysfunction and normal-weight animals with significant metabolic impairments within the same Wistar cohort [18]. This expands the utility of Wistar rats as a model to study diverse metabolic states within a single strain, increasing both translational relevance and experimental efficiency.

Although the commercial diet differs from the experimental diets, it broadly aligns with NRC-95R micronutrient recommendations. Therefore, unexpected effects are unlikely to arise from deficiencies, aside from previously noted ones. All diets share a similar matrix, with approximately 75% of ingredients derived from soy, corn, and wheat, minimizing variability in nutrient availability and metabolic impact[59]. Moreover, the two SP diets were nutritionally matched, supporting the conclusion that metabolic differences stem from processing and macronutrient composition.

CONCLUSION

In summary, this study underscores the pivotal role of dietary composition and food processing in driving metabolic dysfunction, beyond weight and adiposity alone. Although semi-purified diets may promote adiposity and weight gain, the development of MtS and T2D appears to require a diet rich in both fat and sugar. These findings reinforce the fuel partitioning hypothesis and suggest that Impaired

energy utilization plays a more critical role in metabolic disease than fat mass itself. Notably, this is the first report of systemic oxidative changes linked to semi-purified diets in adult male Wistar rats, highlighting the importance of evaluating both macro- and micronutrient profiles when assessing dietary impacts. This work enhances our understanding of obesity-related comorbidities and supports the development of targeted nutritional models for research and clinical applications.

FUNDING

This research received no external funding.

CONFLICTS OF INTEREST

The authors declare no conflicts of interest.

ETHICS APPROVAL

All experimental procedures were conducted in strict adherence to the Ethical Principles in Animal Research endorsed by the Brazilian College of Animal Experimentation and were approved by the Ethics Committee on Animal Use of the State University of Londrina ((Official Letter Nº 074/2022 Protocol Nº 032.2022)

DATA AVAILABILITY

The data supporting the findings of this study are available from the corresponding author upon reasonable request.

AUTHOR CONTRIBUTIONS

Pedro Rocha Tenorio conceived and designed the study, performed all experiments, analyzed the data, and wrote the manuscript. Débora Hipólito Quadreli and Glaura Scantamburlo Alves Fernandes contributed to the oxidative stress assays. Gabriel Smolak Sobieski e Silva assisted with animal care, histological procedures, and manuscript revision. Fábio Goulart de Andrade participated in all phases of the project, acting as the project supervisor. All authors read and approved the final version of the manuscript.

ACKNOWLEDGMENTS

The authors would like to express their sincere gratitude to the *Central Animal Facility of the Center for Biological Sciences, State University of Londrina* for the provision and maintenance of laboratory animals.

REFERENCES

1. NCD Risk Factor Collaboration (NCD-RisC) (2017) Worldwide trends in body-mass index, underweight, overweight, and obesity from 1975 to 2016: a pooled analysis of 2416 population-based measurement studies in 128·9 million children, adolescents, and adults. Lancet 390:2627–2642

2. Okunogbe A, Nugent R, Spencer G, Ralston J, Wilding J (2021) Economic impacts of overweight and obesity: current and future estimates for eight countries. BMJ Glob Health 6:e009773

3. GBD 2019 Diseases and Injuries Collaborators (2020) Global burden of 369 diseases and injuries in 204 countries and territories, 1990-2019: a systematic analysis for the Global Burden of Disease Study 2019. Lancet 396:1204–1222

4. Finkelstein EA, Khavjou OA, Thompson H, Trogdon JG, Pan L, Sherry B, Dietz W (2012) Obesity and severe obesity forecasts through 2030. Am J Prev Med 42:563–70

5. Chan W-K, Chuah K-H, Rajaram RB, Lim L-L, Ratnasingam J, Vethakkan SR (2023) Metabolic Dysfunction-Associated Steatotic Liver Disease (MASLD): A State-of-the-Art Review. J Obes Metab Syndr 32:197–213

6. Ahmed B, Sultana R, Greene MW (2021) Adipose tissue and insulin resistance in obese. Biomed Pharmacother 137:111315

7. Suleiman JB, Mohamed M, Bakar ABA (2020) A systematic review on different models of inducing obesity in animals: Advantages and limitations. J Adv Vet Anim Res 7:103–114

8. Valicente VM, Peng C-H, Pacheco KN, Lin L, Kielb EI, Dawoodani E, Abdollahi A, Mattes RD (2023) Ultraprocessed Foods and Obesity Risk: A Critical Review of Reported Mechanisms. Adv Nutr 14:718–738

9. Speakman JR (2019) Use of high-fat diets to study rodent obesity as a model of human obesity. Int J Obes (Lond) 43:1491–1492

10. Bastías-Pérez M, Serra D, Herrero L (2020) Dietary Options for Rodents in the Study of Obesity. Nutrients 12:3234

11. Kumar V, Singh DD, Lakhawat SS, Yasmeen N, Pandey A, Singla RK (2022) Biogenic Phytochemicals Modulating Obesity: From Molecular Mechanism to Preventive and Therapeutic Approaches. Evid Based Complement Alternat Med 2022:6852276

12. Zhang L, Li X, Liu X, et al (2022) Purified diet versus whole food diet and the inconsistent results in studies using animal models. Food Funct 13:4286–4301

13. Cheng HS, Phang SCW, Ton SH, Abdul Kadir K, Tan JBL (2019) Purified ingredient-based high-fat diet is superior to chow-based equivalent in the induction of metabolic syndrome. J Food Biochem 43:e12717

14. Almeida-Suhett CP, Scott JM, Graham A, Chen Y, Deuster PA (2019) Control diet in a high-fat diet study in mice: Regular chow and purified low-fat diet have similar effects on phenotypic, metabolic, and behavioral outcomes. Nutr Neurosci 22:19–28

15. Shahidi F, Pan Y (2022) Influence of food matrix and food processing on the chemical interaction and bioaccessibility of dietary phytochemicals: A review. Crit Rev Food Sci Nutr 62:6421–6445

16. Del Bas JM, Caimari A, Ceresi E, Arola-Arnal A, Palou A, Arola L, Crescenti A (2015) Differential effects of habitual chow-based and semi-purified diets on lipid metabolism in lactating rats and their offspring. Br J Nutr 113:758–69

17. Parkman JK, Mao X, Dillon K, Gudivada A, Moustaid-Moussa N, Saxton AM, Kim JH (2016) Genotype-dependent Metabolic Responses to Semi-Purified High-Sucrose High-Fat Diets in the TALLYHO/Jng vs. C57BL/6 Mouse during the Development of Obesity and Type 2 Diabetes. Exp Clin Endocrinol Diabetes 124:622–629

18. Preguiça I, Alves A, Nunes S, Fernandes R, Gomes P, Viana SD, Reis F (2020) Diet-induced rodent models of obesity-related metabolic disorders-A guide to a translational perspective. Obes Rev 21:e13081

19. Charan J, Biswas T (2013) How to calculate sample size for different study designs in medical research? Indian J Psychol Med 35:121–6

20. National Research Council (US) Subcommittee on Laboratory Animal Nutrition (1995) Nutrient Requirements of Laboratory Animals: Fourth Revised Edition, 1995. https://doi.org/10.17226/4758

21. Lee H, Um M, Nam K, Chung S-J, Park Y (2021) Development of a Prediction Model to Estimate the Glycemic Load of Ready-to-Eat Meals. Foods. https://doi.org/10.3390/foods10112626

22. Nery C da S, Pinheiro IL, Muniz G de S, Vasconcelos DAA de, França SP de, Nascimento E do (2011) Medidas murinométricas e eficiência alimentar em ratos provenientes de ninhadas reduzidas na lactação e submetidos ou não ao exercício de natação. Revista Brasileira de Medicina do Esporte 17:49–55

23. Ampuero J, Aller R, Gallego-Durán R, et al (2024) The biochemical pattern defines MASLD phenotypes linked to distinct histology and prognosis. J Gastroenterol 59:586–597

24. Aebi H (1984) Catalase in vitro. Methods Enzymol 105:121–6

25. Benzie IF, Strain JJ (1996) The ferric reducing ability of plasma (FRAP) as a measure of “antioxidant power”: the FRAP assay. Anal Biochem 239:70–6

26. Rahman I, Kode A, Biswas SK (2006) Assay for quantitative determination of glutathione and glutathione disulfide levels using enzymatic recycling method. Nat Protoc 1:3159–65

27. Jiang ZY, Hunt J V, Wolff SP (1992) Ferrous ion oxidation in the presence of xylenol orange for detection of lipid hydroperoxide in low density lipoprotein. Anal Biochem 202:384–9

28. Colombo G, Clerici M, Garavaglia ME, Giustarini D, Rossi R, Milzani A, Dalle-Donne I (2016) A step-by-step protocol for assaying protein carbonylation in biological samples. J Chromatogr B Analyt Technol Biomed Life Sci 1019:178–90

29. Erel O (2005) A new automated colorimetric method for measuring total oxidant status. Clin Biochem 38:1103–11

30. Monsanto SP, Hintze KJ, Ward RE, Larson DP, Lefevre M, Benninghoff AD (2016) The new total Western diet for rodents does not induce an overweight phenotype or alter parameters of metabolic syndrome in mice. Nutr Res 36:1031–1044

31. Jin X, Qiu T, Li L, Yu R, Chen X, Li C, Proud CG, Jiang T (2023) Pathophysiology of obesity and its associated diseases. Acta Pharm Sin B 13:2403–2424

32. Ibrahim MM (2010) Subcutaneous and visceral adipose tissue: structural and functional differences. Obes Rev 11:11–8

33. Calderón-DuPont D, Torre-Villalvazo I, Díaz-Villaseñor A (2023) Is insulin resistance tissue-dependent and substrate-specific? The role of white adipose tissue and skeletal muscle. Biochimie 204:48–68

34. Friedman MI, Sørensen TIA, Taubes G, Lund J, Ludwig DS (2024) Trapped fat: Obesity pathogenesis as an intrinsic disorder in metabolic fuel partitioning. Obesity Reviews. https://doi.org/10.1111/obr.13795

35. Lackey DE, Lazaro RG, Li P, Johnson A, Hernandez-Carretero A, Weber N, Vorobyova I, Tsukomoto H, Osborn O (2016) The role of dietary fat in obesity-induced insulin resistance. American Journal of Physiology-Endocrinology and Metabolism 311:E989–E997

36. Barr SB, Wright JC (2010) Postprandial energy expenditure in whole-food and processed-food meals: implications for daily energy expenditure. Food Nutr Res 54:5144

37. Panchal SK, Carnahan S, Brown L (2017) Coconut Products Improve Signs of Diet-Induced Metabolic Syndrome in Rats. Plant Foods Hum Nutr 72:418–424

38. Hou X-D, Qin X-Y, Hou J, Tang H, Ge G-B (2022) The potential of natural sources for pancreatic lipase inhibitors: a solution of the obesity crisis? Expert Opin Drug Discov 17:1295–1298

39. Ćorković I, Gašo-Sokač D, Pichler A, Šimunović J, Kopjar M (2022) Dietary Polyphenols as Natural Inhibitors of α-Amylase and α-Glucosidase. Life (Basel). https://doi.org/10.3390/life12111692

40. Baena M, Sangüesa G, Dávalos A, Latasa M-J, Sala-Vila A, Sánchez RM, Roglans N, Laguna JC, Alegret M (2016) Fructose, but not glucose, impairs insulin signaling in the three major insulin-sensitive tissues. Sci Rep 6:26149

41. Püschel GP, Henkel J (2018) Dietary cholesterol does not break your heart but kills your liver. Porto Biomed J 3:e12

42. Chung S, Parks JS (2016) Dietary cholesterol effects on adipose tissue inflammation. Curr Opin Lipidol 27:19–25

43. Martínez Leo EE, Segura Campos MR (2019) Systemic Oxidative Stress: A key Point in Neurodegeneration - A Review. J Nutr Health Aging 23:694–699

44. Świątkiewicz I, Wróblewski M, Nuszkiewicz J, Sutkowy P, Wróblewska J, Woźniak A (2023) The Role of Oxidative Stress Enhanced by Adiposity in Cardiometabolic Diseases. Int J Mol Sci 24:6382

45. Newaz MA, Nawal NN (1998) Effect of alpha-tocopherol on lipid peroxidation and total antioxidant status in spontaneously hypertensive rats. Am J Hypertens 11:1480–5

46. Caetano AC, da Veiga LF, Capaldi FR, de Alencar SM, Azevedo RA, Bezerra RMN (2013) The antioxidant response of the liver of male Swiss mice raised on a AIN 93 or commercial diet. BMC Physiol 13:3

47. Dominko K, Dikic D, Hecimovic S (2020) Enhanced activity of superoxide dismutase is a common response to dietary and genetically induced increased cholesterol levels. Nutr Neurosci 23:398–410

48. Rindler PM, Plafker SM, Szweda LI, Kinter M (2013) High dietary fat selectively increases catalase expression within cardiac mitochondria. J Biol Chem 288:1979–90

49. Russo E, Leoncini G, Esposito P, Garibotto G, Pontremoli R, Viazzi F (2020) Fructose and Uric Acid: Major Mediators of Cardiovascular Disease Risk Starting at Pediatric Age. Int J Mol Sci 21:4479

50. Arivazhagan L, López-Díez R, Shekhtman A, Ramasamy R, Schmidt AM (2022) Glycation and a Spark of ALEs (Advanced Lipoxidation End Products) - Igniting RAGE/Diaphanous-1 and Cardiometabolic Disease. Front Cardiovasc Med 9:937071

51. Zazula MF, Saraiva DF, Theodoro JL, et al (2023) An Early and Sustained Inflammatory State Induces Muscle Changes and Establishes Obesogenic Characteristics in Wistar Rats Exposed to the MSG-Induced Obesity Model. Int J Mol Sci. https://doi.org/10.3390/ijms24054730

52. Ullah R, Rauf N, Nabi G, Yi S, Yu-Dong Z, Fu J (2021) Mechanistic insight into high-fat diet-induced metabolic inflammation in the arcuate nucleus of the hypothalamus. Biomed Pharmacother 142:112012

53. Karaca M, Martin-Levilain J, Grimaldi M, Li L, Dizin E, Emre Y, Maechler P (2018) Liver Glutamate Dehydrogenase Controls Whole-Body Energy Partitioning Through Amino Acid-Derived Gluconeogenesis and Ammonia Homeostasis. Diabetes 67:1949–1961

54. Lee J, Kim J, Lee R, et al (2022) Therapeutic strategies for liver diseases based on redox control systems. Biomed Pharmacother 156:113764

55. Magkos F, Fabbrini E, Mohammed BS, Patterson BW, Klein S (2010) Increased whole-body adiposity without a concomitant increase in liver fat is not associated with augmented metabolic dysfunction. Obesity (Silver Spring) 18:1510–5

56. Jakubiak GK, Osadnik K, Lejawa M, Kasperczyk S, Osadnik T, Pawlas N (2021) Oxidative Stress in Association with Metabolic Health and Obesity in Young Adults. Oxid Med Cell Longev 2021:9987352

57. Di Renzo L, Galvano F, Orlandi C, Bianchi A, Di Giacomo C, La Fauci L, Acquaviva R, De Lorenzo A (2010) Oxidative stress in normal-weight obese syndrome. Obesity (Silver Spring) 18:2125–30

58. Zhou Z, Macpherson J, Gray SR, Gill JMR, Welsh P, Celis-Morales C, Sattar N, Pell JP, Ho FK (2021) Are people with metabolically healthy obesity really healthy? A prospective cohort study of 381,363 UK Biobank participants. Diabetologia 64:1963–1972

59. van den Berg LA, Mes JJ, Mensink M, Wanders AJ (2022) Protein quality of soy and the effect of processing: A quantitative review. Front Nutr 9:1004754